Energy & Environmental Science

Accepted Manuscript

ROYAL SOCIETY OF CHEMISTRY

www.rsc.org/ees

Broader Context for

Oligomeric-Schiff bases as negative electrodes for Sodium Ion Batteries: Unveiling the Nature of their Active Redox Centers

The current and increasing demand of energy makes the use of renewable energy sources essential. To fully utilize and integrate the intermittent renewable sources, such as sun or wind, stationary energy storage in peak hours is needed. We aim at energy storage being cost effective and environmentally sustainable. This requires the development and understanding of battery chemistries from earth abundant low cost raw materials, which can be easily synthesised. We are reporting in here the development of new sustainable oligomeric materials which are synthesised through simple condensation reactions. The new electroactive compounds are hybrids of carboxylate monomers and polymeric-Schiff bases. They act as negative electrodes in sodium ion batteries and can reach voltages of reaction as low as 0.3V *vs.* Na^+/Na. Electrode optimization led to reversible capacities as high as 340mAh/g, which makes them candidates for next generation of environmental friendly sodium ion batteries.

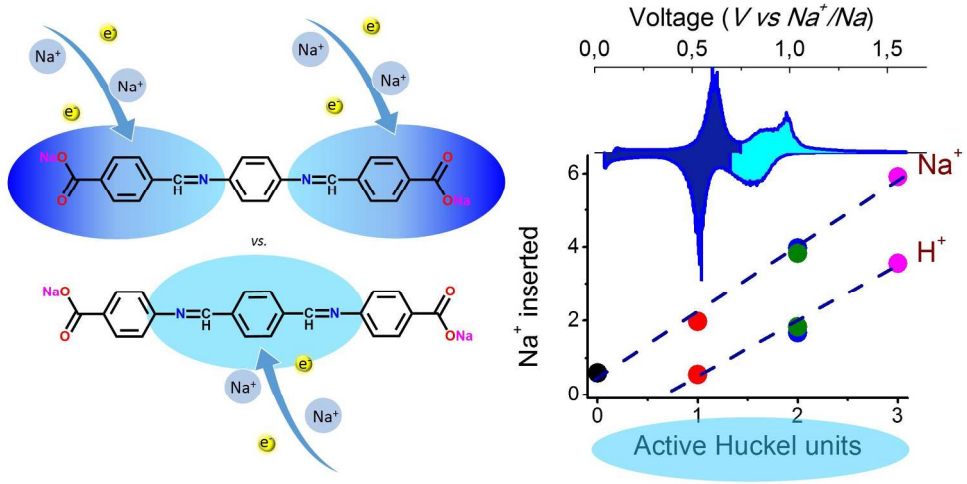

Novel oligomers, hybrids between Carboxylate and Schiff base aromatic functionalities, show reversible sodium insertion below 1V vs Na+/Na. Understanding of the redox active units enables design of low cost, safe and environmentally friendly anode materials.
412x210mm (150 x 150 DPI)

Oligomeric-Schiff bases as negative electrodes for Sodium Ion Batteries: Unveiling the Nature of their Active Redox Centers

María López-Herraiz [a], Elizabeth Castillo-Martínez [a] *, Javier Carretero-González [a,§], Javier Carrasco [a], Teófilo Rojo [a,b], Michel Armand [a] *

[a] CIC EnergiGUNE, Alava Technology Park, C/Albert Einstein 48, 01510, Miñano, Alava, Spain.

[b] Departamento de Química Inorgánica, Universidad del País Vasco UPV/EHU, P.O. Box 664, 48080 Bilbao, Spain.

[§] Current address: Polymer Ionics Research Group, Warsaw University of Technology, 3 Noakowskiego, 00-664, Warsaw, Poland.

*Corresponding authors: ecastillo@cicenergigune.com, michel.armand@gmail.com

ABSTRACT

Oligomeric Schiff bases with carboxylate end groups are crystalline, electrochemically active materials at voltages below 1 V vs. Na^+/Na. This low redox voltage along with delivered capacities up to 340 mAh/g makes them potential anode materials for sodium ion batteries. The electrochemical performance is optimized by maximizing the number of active units with respect to the total chain length. We report for the first time the

electrochemical activity of the 10-π-electrons end group (–$^{-}$OOC-ϕ-C=N–) (ϕ refers to phenyl group) and central (–N=C-ϕ-C=N–) Hückel units. This enhanced activity is due to the larger stability of planar molecular regions with respect to out-of-plane inactive (–$^{-}$OOC-ϕ-N=C–) and (–C=N-ϕ-N=C–), as confirmed by DFT calculations.

INTRODUCTION

The large and increasing demand for energies with low CO_2 footprint has prompted intense research and development of low cost and sustainable electrochemical energy storage systems. While lithium (Li)-ion batteries dominate the portable consumer electronics market, due to their high energy density, problems arise when trying to use them in large storage application due to the high cost and geographical restrictions of lithium ores. To tackle those problems, sodium, a low cost and abundant element, is emerging as a replacement of the lithium vector in Na-ion batteries (SIB)[1]. In addition, on the positive electrode, abundant Fe- or Mn-based oxides can replace rare Ni- and Co-based ones, which are much less environmentally friendly. Conversely, for negative electrode materials, with the exception of sodium titanates in the inorganic world , ($Na_{2+x}Ti_3O_7$ or lepidocrocite-structured titanates[2,3,4], organics provide a wide molecular and structural diversity and flexibility, the possibility of tuning the redox potentials, multi-electron reactions, great abundance and they are easy to recycle[5,6].

Conjugated polymers such as Polyacetylene and polyphenylene[7] showed reversible sodium and lithium ion intercalation at voltages low enough to behave as anodes for SIB and LIB already in 1985. However, their low diffusion coefficients for ion migration and large structural rearrangements (probably involving solvent-cointercalation) prevented their further development at that time. Recently, conjugated dicarboxylates, mainly the alkali salts of terephthalates and higher homologues, have

emerged as active materials for both LIB and SIBs at ≈ 0.3V vs Na^+/Na. [8,9,10,11,12] These conjugated carboxylates are electrochemically active by virtue of the additional insertion of lithium/sodium in the –COOLi/Na unit, which is reduced to $–C(OLi/Na)_2$. The already present lithium/sodium ions do not participate in the electrochemical reactions. Additionally, N/O-containing functionalities have been explored: disodium pyromellitic diimidate,[13] as well as indigo carmine[14] or pteridine based electrodes,[15] operate at average voltages of 1, 2 and 2.5 V vs. Na^+/Na respectively but their equivalent weight is relatively high. Our group recently reported polymeric Schiff-bases as active anode materials,[16] which can insert sodium at voltages as low as 0.65 V vs Na^+/Na with up to 350 $mAhg^{-1}$ of capacity. The 10-π electrons unit -N=CH-ϕ-CH=N-, is capable of inserting more than one sodium ion per –C=N- bond and is responsible for the observed electrochemical activity. The mentioned unit, -N=CH-ϕ-CH=N-, obeys the Hückel rule of aromaticity, which states that cyclic coplanar units which contain (4n+2)π electrons (n=1, 2…) gets extra stability. The isoelectronic inverse unit, -HC=N-ϕ-N=CH-, however was shown to be electrochemically inactive, which was ascribed to the loss of planarity of the group due to the strong electronic interaction between the unpaired electrons of the N and the π electron cloud of the adjacent aromatic ring. Unsubstituted aromatic poly-schiff bases showed two redox processes which we assigned to two one-electron reactions as described by Martinet et al. for benzylideneaniline in DMF solution.[17] They proposed that the first electron forms a radical anion in equilibrium between the azo and carbo radical (involving dimerization), and the second electron yields the dianion.

It would be interesting to hybridize this type of redox active material with the carboxylate family as they show high capacity and processable liquid-crystalline materials may be obtained with extensive π - π interactions. In this paper, oligomeric

Schiff-bases are introduced as novel organic anode materials for low-cost SIB. The oligomers possess a core with variable number and orientation of aromatic azomethine-based active Hückel units and they are all terminated by carboxylate groups. We rationalize the dependence of the specific capacity on the molecular structure of these compounds using first-principles insight.

Synthesis of oligomeric Schiff bases. Oligomeric Schiff bases were synthesized by condensation reaction from aromatic monosubstituted amines (*Aldrich,* 4-Aminobenzoic acid) or bisubstituted amines (*Aldrich*, p-phenylendiamine) and aromatic or aliphatic monosubstituted aldehydes (*Aldrich*, 4-formyl benzoic acid or pyruvic acid) or bis- aldehydes (*Aldrich*, terephthalaldehyde)). Stoichiometric amounts of the reactants were used, without any further purification, being dispersed separately in toluene (*Aldrich*) for 10 min. The desired dispersed reactants were mixed in a closed vial and left reacting for 24 hours at 85°C. The solution was filtered while hot and the collected colored solid was dried at 80°C. **Sodiation of oligomeric Schiff bases.** Oligomeric-Schiff bases were sodiated by ion-exchange reaction using a sodium salt (*Aldrich*, sodium thiocyanate) and a base (*Aldrich*, Triethylamine). The protonated monomer and the sodium salt were dispersed separately in acetonitrile (*Aldrich*) in a proportion 1:4. Both solutions were mixed and the base was added in a proportion 1:2 with respect to the monomer. The mixture reacted for 24 hours at 45°C. The collected solid was washed 3 times with acetonitrile using centrifugation at 4000 rpm for 10 min each time. **Characterization of oligomeric Schiff bases.** Infrared spectra were recorded using a Perkin Elmer FTIR Spectrum 400 DTGS spectrometer in the range of ν=4000-450 cm^{-1} by preparing KBr pellets. Powder X-ray diffraction data of dried powdered samples were collected using a Bruker Advance D8 instrument with copper K alpha radiation ($CuK\alpha_{1,2,}$ λ=1.54056 Å) in the range 2Θ=4-80 degrees with a step size

of 0.029 degrees. STA measurements were performed using a NETZSCH STA 449 F3 apparatus heated until 550°C at 10K/min. **Electrochemical behavior in Sodium ion batteries.** The electrochemical performance vs metallic sodium was measured in CR 2032 coin cell containing hand milled powder mixtures: 80% wt. active material, 15% wt. Carbon Super C-65 (Imerys) and 5% wt. Ketjen Black (Imerys). Glass fiber Whatman GFB/55 was used as separator and 1M NaFSI (*Solvionic*) in Me-THF (*Aldrich*) as electrolyte. Typical electrode masses were 2.4-4 mg of active material. Galvanostatic measurements were run in a MACCOR battery tester at different c-rates considering the theoretical capacity as that corresponding to the insertion of $1Na^+$/–C=N or $–C=OO^-$ group linked to an aromatic ring. Theoretical capacities for each oligomer are listed in Table S2. They range between 161 and 288 mAh/g. Therefore specific current densities were 16-29 mA/g for C/10, 32-58 mA/g for C/5 and 161-288 mA/g for 1C. As the area of the electrode was not constant, due to the electrode being a dispersed powder, areal current densities were not calculated.

RESULTS and DISCUSSIONS

Synthesis: The Schiff bases oligomers synthesized and characterized in this work are presented in *Figure 1*. They are all synthesized by condensation reaction between mono ($X \neq –NH_2$) or bi-substituted ($X = –NH_2$) aromatic amines and mono ($Y \neq –CHO$) or bi-substituted ($Y \neq –CHO$) aliphatic or aromatic aldehydes, all in para positions. Short oligomers (O1, O2, O3) form when reacting stoichiometric amounts of 2 reactants while longer chain oligomers are formed with 3 different reagents. From this reaction the 'protonated oligomers' are produced. These crystalline solids (Figure S1) are further ionically exchanged with an easily soluble sodium salt, sodium thiocyanate, NaSCN, in presence of an organic base, resulting in the formation of the 'sodiated oligomers' with sodium as counter cation; the by-product Et_3NH^+,SCN^- being easily separated in the

supernatant after centrifugation. The colors range from brown (O1) to a variety of shades of yellow (O2-O5). All target oligomers are symmetric so that a more stable radical can be stabilized at intermediate steps of electrochemical sodium insertion.[18]

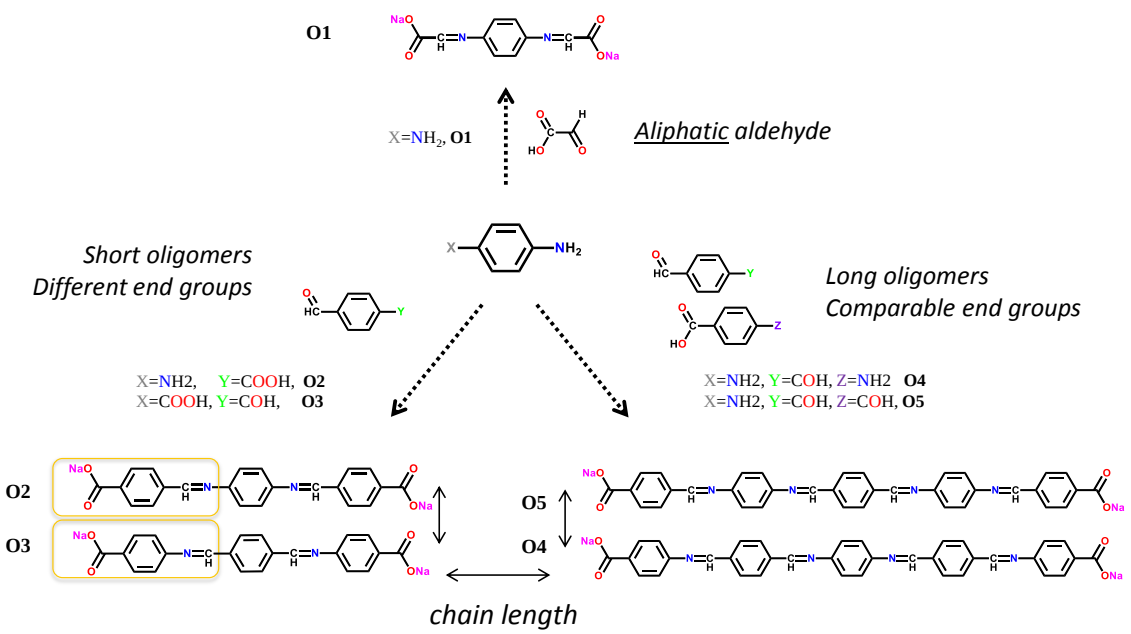

Figure 1. Oligomeric Schiff-bases prepared by condensation reaction of di/aldehydes and aromatic amines. The byproduct of the reaction is water.

Characterization: The formation of the imine bond –CH=N-R is ensured by the appearance of a stretching band in the FTIR spectra of all the oligomers at ~1611-1622 cm^{-1} (Figure S2 and Figure 2(a)). The vibration frequencies of this group are lowered by conjugation with the rest of the phenyl rings in the chain, appearing at higher frequencies, 1650 cm^{-1}, in the non-conjugated oligomer, O1 (Table 1). The ionic exchange step is confirmed by the almost complete disappearance of the stretching band at ~1670-1686cm^{-1}, corresponding to the carboxylic acid (–COOH) group[19], and the subsequent appearance of two new bands, attributed to the asymmetric and symmetric vibration bands of the carboxylate, (–COO^{-}) group at ~1530-1540 cm^{-1} and ~1387-1411 cm^{-1} respectively (Figure 2(a)). This exchange does not seem complete for O1Na.

Being the only amorphous oligomer, its exchange ability might be quite different from that of other oligomers, for which the ionic exchange has been optimized.

Table 1. Characteristic features of the studied oligomeric Schiff bases. Molecular structure, color, Infrared frequencies corresponding to the main vibration bands for the oligomers synthesized in the present work.

	X	Colour	ν(C=N)	ν(C=OOH)	ν(C=OO-) asym	ν(C=OO-) sym
O1	H^+	brown	1650	1670		
	Na^+		1650		1520	1387
O2	H^+	Yellow-green	1620	1686		
	Na^+		1620		1539	1410
O3	H^+	Light yellow	1622	1679		
	Na^+		1622		1539	1400
O4	H^+	Yellow-orange	1619	1679		
	Na^+		1615		1540	1403
O5	H^+	Yellow-orange	1613	1686		
	Na^+		1613		1537	1411

All the synthesized oligomeric Schiff-bases are crystalline with the exception of O1, which is amorphous, both in its protonated and its sodiated forms (Figure S1 and Figure 2(b) respectively). In addition, protonated oligomers of the same length show similar PXRD patterns (Figure S1), e.g. O2H vs O3H, regardless of the –CH=N- orientation with respect to the end group. This indicates that the crystal packing is dominated by the π stacking of the phenyl rings and available intermolecular hydrogen bonds among the ending groups of the molecules; intermolecular H-bonds with the N atoms of azomethine groups are therefore unlikely, since they would lead to differences on the PXRD patterns of O2H vs O3H and O4H vs O5H. Sodiated oligomers are less

crystalline than the protonated forms and the PXRD patterns of oligomers of the same length become more distinct. (Figure 2(b)).

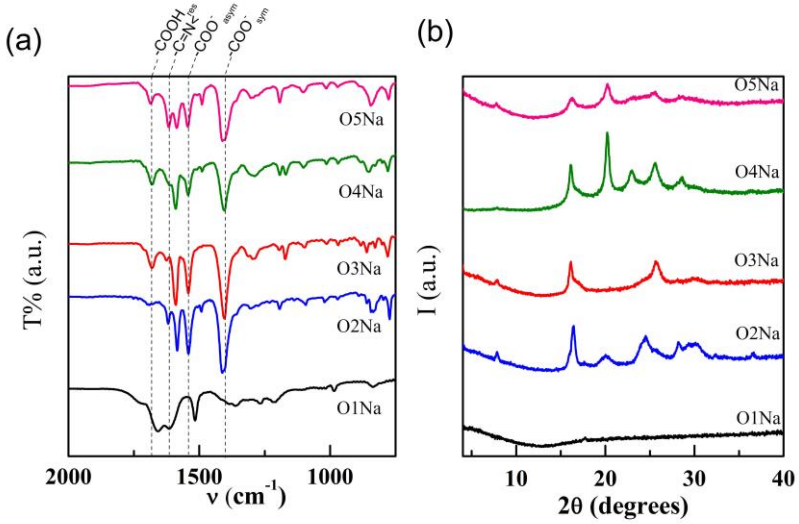

Figure 2. Characterization of the oligomers in their sodiated form (a) FTIR spectra showing the bands corresponding to the carboxyl (-COOH), imine (-C=N) and carboxylate (-COO-) groups with a dashed line (b) PXRD patterns.

We performed a detailed solubility study to find a suitable solvent, which can dissolve the oligomers and also enable their characterization by liquid NMR, Table S1. The oligomers are insoluble[20] in non-polar solvents (toluene) and they are only partially soluble in aprotic polar solvents (DMSO, DMF or NMP) or even in protic polar solvents (glacial acetic acid). Interestingly, when the carboxylic groups are transformed into the salt form, as it happens after the ionic exchange, all the oligomers become soluble in water, however liquid ^{1}H-NMR of O2Na dissolved in D_2O showed that a small degree of hydrolysis takes place (Figure S3).

Another key observation is the change of color when O2Na and O5Na are dissolved in water (Figure S4). The initial yellowish solution becomes brownish and remains brown upon drying. This only occurs on the oligomers that have the same Hückel group configuration, $^{-}$-OOC=CH-ϕ-CH=N-, but it is not observed for oligomers with the inverse configuration, O3-Na and O4-Na. The recovered brownish dried powder was

characterized by PXRD (Figure S5) and FTIR. The FTIR spectra indicate that the functional groups were maintained, which discards hydrolysis, but slight changes in the intensities of some reflections of the PXRD pattern suggests a possible change from a metastable phase obtained during the dispersion-based ionic exchange, to a more stable packing after dissolution in water.

The thermal stability of the prepared oligomers was also studied by Simultaneous Thermal Analysis (STA) experiments in air and argon atmosphere so as to evaluate its possible use or processing as electrodes at relatively high temperature. TG curves show the high thermal stability of all the oligomers with a mass loss of 0-10% for protonated oligomers and 0-5% for the sodiated oligomers at 300°C, (Figure S6 and S7) and ~40% loss for the protonated *vs* ~20% for the sodiated oligomers at 500°C in argon. The higher thermal stability of sodiated oligomers is probably due to stronger 3D intermolecular interactions induced by the Na^+ ions.

Electrochemical performance: Galvanostatic experiments in the 0.05-1.6 V range vs Na^+/Na were performed for both protonated and sodiated forms at currents of C/10 ($C=1Na^+$/-C=N or $–COO^-$ which results in 16-29mA/g). Figure S8 and Figure 3 show the first and second reduction and oxidation respectively. All oligomers show quite large first cycle reduction capacity (Figure S8) which is not recovered upon the first oxidation. This large irreversible capacity suggests electrolyte decomposition and formation of a solid-electrolyte interface (SEI). Not very large BET surface areas of 7 m^2/g for O2Na and 24 m^2/g for O2H suggest that there might be additional contributions to the irreversible capacity, such as secondary reactions of a possibly radical anion formed during the first electron reduction reaction.[21] The coulombic efficiency is thus very small (20%) the first cycle and then rapidly increases to 98%. The oligomer prepared from the aliphatic aldehyde, O1Na, shows the smallest

reversible capacity, probably due to lower activity (not shown in Figure 3a). All other protonated and sodiated oligomers show at least one pseudo-plateau in the voltage range 0.05-1.6V; they are therefore electrochemically active at the desired voltage for negative electrode operation in sodium ion batteries. However, we found a very large dependence of the capacity and voltage of the redox processes on the molecular structure. A summary of the most relevant electrochemical data is listed in Table S2. Figure 3a shows the derivative of the capacity *vs* voltage for the protonated and sodiated forms of oligomer O2. The protonated phase O2H shows two redox peaks at 0.65 and 0.97 V vs Na^+/Na for oxidation, whereas the sodiated phase O2Na have 3 redox peaks at 0.62, 0.90, and 1.01 V vs Na^+/Na for oxidation (Table S2). In addition, O2Na derivative peaks are more intense than O2H peaks. This implies that the protonated phases are electrochemically different active materials, and protons are not being simply replaced by sodium ions during cycling.[22] On the contrary, different redox reactions occur in both sodiated and protonated forms of the same oligomer. As deduced from the larger intensity of the $\partial Q/\partial V$ peaks of O2-Na with respect to O2-H (Figure 3a), sodiated oligomers show higher capacities than their protonated parent counterparts. This might be due to the fact that hydrogen bonding of carboxylates leaves a smaller space available for sodium insertion than that left after the packing imposed by the typical six-fold coordination of sodium ion[23] in organic carboxylate salts.

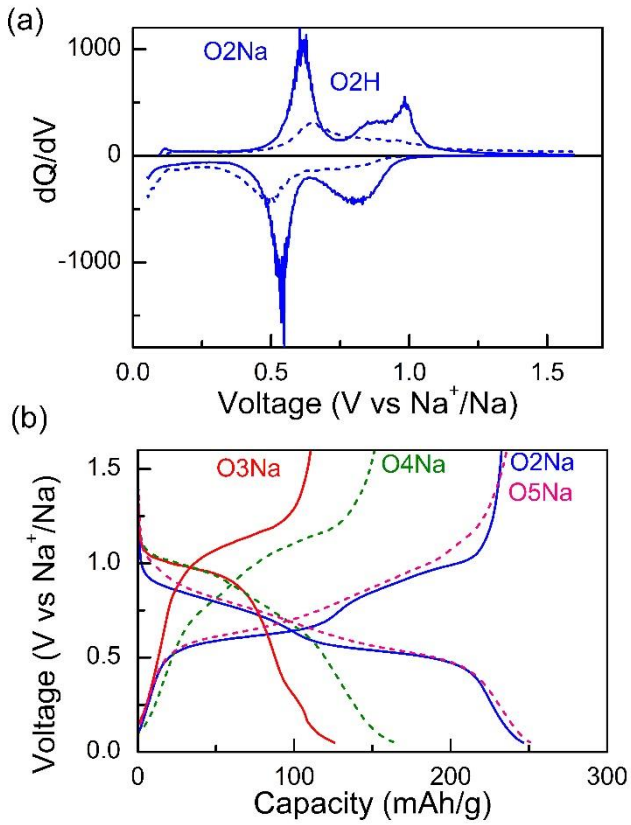

Figure 3. (a) Voltage derivatives of the specific capacity vs. voltage for the second reduction and oxidations for protonated (dashed) and sodiated (solid) oligomeric Schiff bases O2. **(b)** Voltage vs. specific capacity for the 2nd galvanostatic reduction and oxidation of the sodiated oligomers O2-Na, O3-Na, O4-Na and O6-Na. In all cases active materials are mixed with 15% carbon Super C-65 and 5% ketjen black and galvanostatically discharged at C/10 being C=1 Na^+ ions/-C=N or $–COO^-$ in 10 hours

The capacity not only depends on the cation, H^+ or Na^+, counterbalancing the charge of the carboxylate end groups, but also on the configuration (orientation) of the azomethine groups with respect to the end carboxylate groups, and to a lesser extent on the chain length. As seen in Figure 3b the sodiated oligomers with the $–^-OOC$-ϕ-CH=N- end group (O2 and O5) have higher reversible capacity, 250 mAh/g, than those with the inverse >C=N- unit and same length (120 mAh/g for O3Na and 170 mAh/g for O4Na) in which sodium ion insertion also seems to occur at higher voltages.

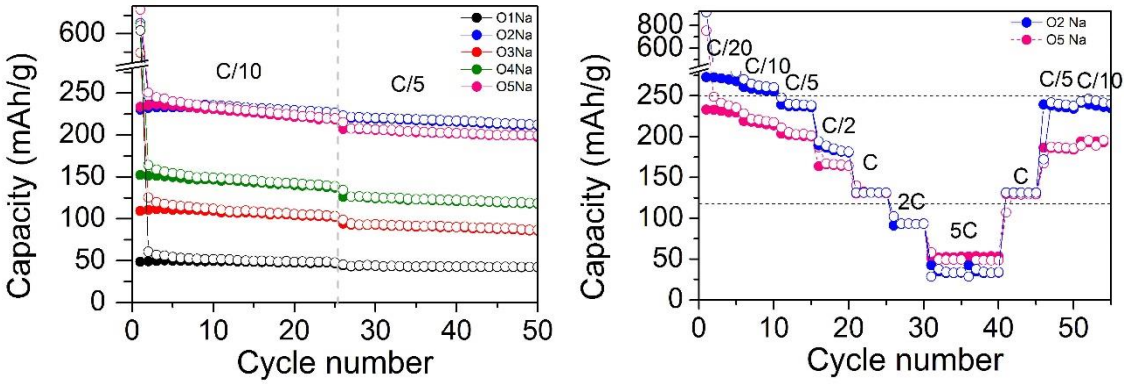

Figure 6

Figure 4. (a) Cyclability for oligomers O1-O5 in their sodiated forms, (b) rate capability for 5 cycles at C/20, C/10, C/5, C/2, C, 2C, 5C, C and C/5 for O2Na (blue) and O5Na (pink).

Figure 4 shows the cycling and rate capability for the sodiated oligomers. The good cyclability and small capacity loss of all the oligomers are remarkable despite having been measured in powdered form. In the case of O2Na, the oligomer with the best electrochemical performance, the capacity retention is 97.5% after 25 cycles at C/10 and 92% after 25 more cycles at C/5. This value is hardly achieved when using many other organic materials due to well-known capacity fading problems.[24] The excellent capacity retention of O2Na can be attributed to the high structural stability of oligomers and to their low solubility in the electrolyte, NaFSI in Me-THF. Comparing the rate capability of the two oligomers with higher capacity, O2-Na and O5-Na, the latter seems to be less affected by the increase of rate.[12]

In order to compare the redox processes occurring in oligomers with each end group, the voltage derivative of the capacity versus the voltage ($\partial Q/\partial V$) for the second reduction and oxidation, are plotted and compared to that of the fully aromatic unsubstituted polymeric Schiff base[16] in Figure 5.

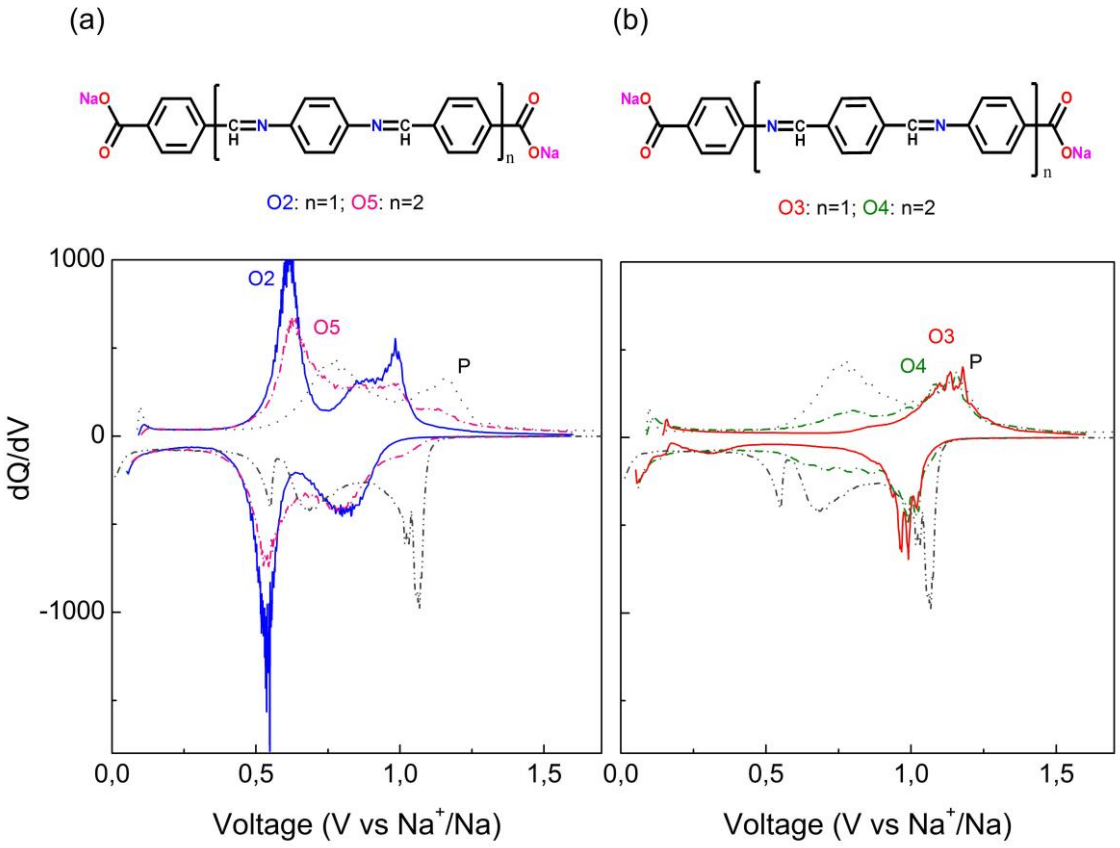

Figure 5. Voltage derivatives of the specific capacity vs voltage for the second reduction and oxidations of Oligomeric Schiff bases (a) with the NaOOC-ϕ-CH=N- end group and (b) with the NaOOC-ϕ-N=CH- end group. The plot for the polymeric Schiff bases is added in dots for comparison and labelled as P. In all cases active materials are mixed with 15% wt. carbon Super C-65 and 5% wt. Ketjen Black and galvanostatically discharged at C/10 (being C=1 Na^+ ions per –C=N or –C=OO–$^-$ unit bonded to an aromatic ring in 1 hours).

The reduction and oxidation of both O2-Na and O5-Na have two common redox processes at 0.45 and 0.80 V (reduction) and 0.65 and 1.00 V (oxidation) vs Na^+/Na (Table S2). We attribute the low voltage reversible process (0.45, 0.65 V vs. Na^+/Na) to the coordination of Na^+ ions with the carboxylic group or with the aromatic ring linked to it, as in graphite intercalation compounds, since it occurs at lower voltages than the redox process of the active unit found in the polymer. Being the carboxylate anion an electron donor, its presence leads to a lowering of the redox voltage of the aromatic active unit. This process is not favored when the monomers have the –$^-$OOC-ϕ-N=C–

ending group, O3-Na and O4-Na, as no low voltage redox process is observed. For O3Na and O4Na, the two reversible processes at 0.79 and 0.990 V (reduction) and 0.81 and 1.1 V (oxidation) (Figure 5(b)) suggest the insertion of Na^+ ions into the active center –N=C-ϕ-C=N-, similar to the one found in the polymer Schiff base. While in poly-Schiff bases, the –N=C-ϕ-CH=N– was reported as the electrochemically active unit,[16] and the inverse and isoelectronic unit is inactive, in the case of the oligomers O1-O5, the group –$^-$OOC-ϕ-CH=N– is also clearly more favorable for the electrochemical sodium insertion compared to –$^-$OOC-ϕ-N=CH–.

Geometrical effects can help to rationalize these findings. Ultimately, the co-planarity of –$^-$OOC-ϕ-CH=N– and –$^-$OOC-ϕ-N=CH– groups determines if they are conjugated and, therefore, can effectively contribute to the electrochemical capacity. Interestingly, X-ray structural studies of crystalline[25] and gas-phase[26] benzylideneaniline both showed that the aniline ring lies significantly out of the C–N=C–C plane. This would suggest a co-planar configuration only for ϕ–CH=N and thus the observed enhanced electrochemical activity over ϕ–N=CH units. In order to confirm this, we carried out a series of density functional theory (DFT) calculations (see Supporting Information for details) to determine the relative stability of different conformations of O2 and O3 gas-phase molecules (Table S3) as a function of the dihedral angles α and β between N=C–C and C–N=C planes (Figure S15). For O2 molecules, we found that the most stable configuration (α=40.4°, β=217.6°) is indeed 77-94 meV more stable than the fully relaxed planar isomers (α=0.1°, β=179.3°; and α=0.3°, β=0.5°). Similarly, planar O3 molecules are less favorable than the most stable isomer (α=320.0°, β=219.6.3°) by at least 130 meV (Table S3). Our DFT results thereby confirm that non-planar ϕ–N=CH units are energetically preferred: twisting out the N=C–C and C–N=C planes by about

40°-45° stabilizes these molecules. In contrast, we found that breaking the planarity of ϕ–CH=N groups is strongly unfavorable (Figure 6). Overall, this implies that only ϕ–CH=N units are π-conjugated, whereas ϕ–N=CH units are not.

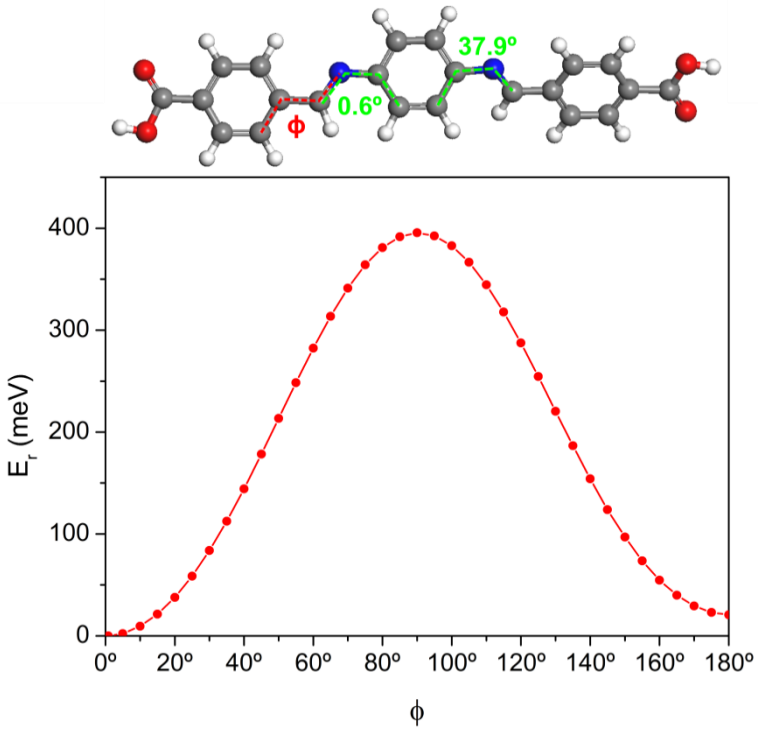

Figure 6. Relative energy (E_r) of O2 gas-phase conformers as a function of the dihedral angle ϕ. Each dot corresponds to a single point calculation at a given ϕ angle, but keeping the molecule frozen at its initial optimal geometry. The connecting lines are merely a guide to the eye. E_r is defined with respect to the conformation (α=0.6°, β=37.9°) in Table S2.

In the case of O2 molecules, the C atom of the ϕ–CH=N group is located next to the ending phenyl ring and, according to our DFT calculations, it is coplanar with it. On the other hand, the ϕ–CH=N group in O3 is not coplanar with the ending phenyl ring but with the middle one, due to the interactions of the free pair of electrons in the N atom (sp^2) and the π electrons of the phenyl ring[25].

In addition, the –$^{-}$OOC-ϕ-CH=N- unit in a O2 molecule contains 10-π electrons and, therefore, obeys the Hückel rule of aromaticity. We will turn to the implications of this again later.

Another key observation is that by increasing the oligomer length the redox peaks shift to higher voltages when comparing O2 and O5 curves in Figure 5(a) but to lower voltages when going from O3 to O4. This is because in O2 molecules only carboxylate based units ($^{-}$–OOC-ϕ-CH=N–) are active, with pure carboxylates being active at lower voltages. When moving from O2 to O5 there is therefore a transition from electrochemically active units based on carboxylates for short oligomers (O2) to these and poly-Schiff bases for longer ones (O5). In contrast, comparing now O3 and O4 molecules (Figure 5(b)), whose active units are only the central –N=CH-ϕ-CH=N– group present also in poly-Schiff bases, there is no change in the active unit; we just observed a small difference in the ring substituents close to these groups and, therefore, the redox peaks are only slightly shifted to lower voltages upon increasing the chain length. This indicates that the control over voltages between those of pure carboxylates and pure poly-Schiff bases is possible.

Proposed model: Normalizing the capacities of all the oligomers to the amount of sodium ions inserted per formula unit, and relating it to the number of active coplanar Hückel units identified by DFT calculations, it is possible to rationalize the effect of the molecular structure on the Na^{+} ion storage capacity (Table 2). First, there is a two-fold increase in the number of Na^{+} ions inserted within the same oligomer when it is sodiated (Table S2), which is likely related to the available space. Second, when

comparing oligomers of the same length (i.e., O2 with O3 and O4 with O5), Na^+ insertion is noticeably enhanced for O2 and O5 oligomers. Those oligomers contain "coplanar" ending groups and, therefore, have a larger ratio of active Hückel units contributing to the capacity than O3 and O4 oligomers. As a consequence, in the case of the oligomers with coplanar ending group, capacity does not increase when increasing the chain length, since the ratio of active/total number of Hückel units remains almost constant. However, capacity does increase when comparing oligomers with non-planar ending groups, where this ratio increases. Therefore, reversible capacity is related (among other aspects like crystallinity and conjugation) with the number of "active" Hückel units (-$^-$OOC-ϕ-C=N- or –N=C-ϕ-C=N-) per total number of units within an oligomer. We listed this ratio in Table 2.

Table 2. Number of Hückel units in different sodiated oligomers and their contribution to reversible capacity. Active Hückel groups considered: -$^-$OOC-ϕ-C=N- (end) and –N=C-ϕ-C=N- (central). Inactive Hückel groups considered: -$^-$OOC-ϕ-N=C- (end) and –C=N-ϕ-N=C- or simply -ϕ- (central).

Oligomer	Hückel units	Active Hückel groups		Inactive Hückel groups	Hückel units contributing to capacity/ total number	Experimental Capacity	Experimental Nº Na ion per active Hückel unit
		end -OOC-ϕ-C=N-	central –N=C-ϕ-C=N-	-OOC-ϕ-N=C- –C=N-ϕ-N=C-			
O2	3	2		1	2/3	278	1.98
O3	3		1	2	1/3	110	1.87
O4	5		2	3	2/5	150	1.91
O5	5	2	1	2	3/5	260	1.97

We found a linear correlation between the total number of Na^+ ions inserted per oligomer and the number of active Hückel groups within each oligomer (Figure S10): increasing the number of active Hückel groups results in the increase of inserted Na^+

ions, as each active Hückel unit is capable of inserting 2 Na^+ ions (Table 2). However, given the fact that a similar slope is observed for the sodiated and the protonated species, the role of the crystal packing and available space in reversible capacity remains unclear.

Considering this model based on the active/total ratio of Hückel units, we performed further experiments as an attempt to both corroborate this hypothesis as well as trying to improve the present results. In order to increase the ratio between active and total Hückel groups, two extra oligomers were synthesized maintaining the favored planar ending group but eliminating the inactive Hückel central rings (**Figure** 7(a)). 4-formyl benzoic acid was reacted with ethylenediamine (O6) or hydrazine (O7) following the same procedure and in a proportion 2:1 in both cases, and followed by ionic exchange to substitute H^+ by Na^+. Performing Galvanostatic cycling of the crystalline (Fig S11) sodiated oligomers O6Na and O7Na did not show an increase in the reversible capacity despite the ratio of active Hückel groups/total Hückel groups was increased to 1 (**Figure** 7(b)).

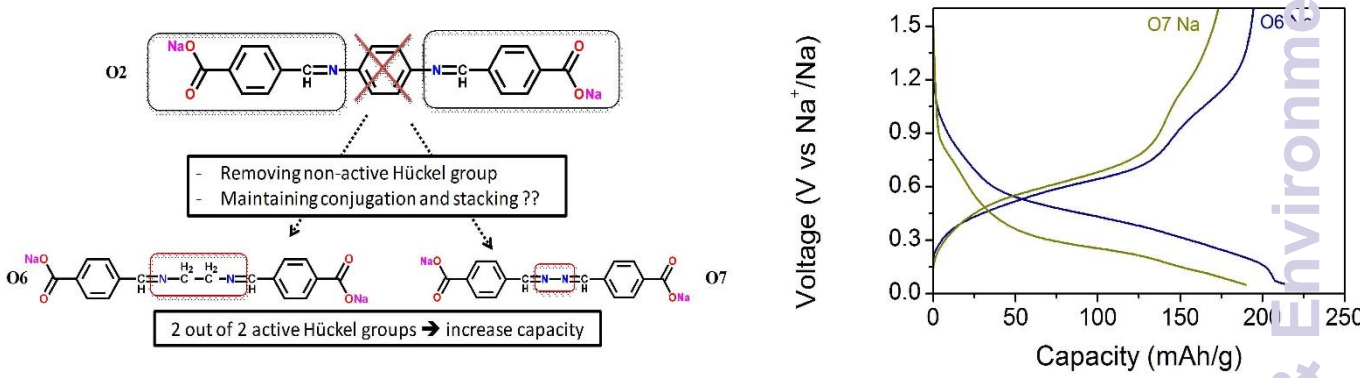

Figure 7.(a) Scheme showing the molecular structure for O6Na and O7Na oligomers. (b) Voltage vs specific capacity for the 2nd galvanostatic reduction and oxidation of the O6Na and O7Na oligomers mixed with 15% Super C-65 and 5% Ketjen black and galvanostatically discharged at C/10 being C=2Na^+ ions/monomer unit in 10 hours).

The reversible capacity remained at a value of 196 mAh/g at C/10, corresponding to Na^+/C=N for the first few cycles in the case of O7Na (**Figure** 7(b)). After that, a drop in capacity gradually occurred until a constant value of 100mAh/g was reached after 10 cycles. From there on, a good stability in the capacity was obtained, even at higher C-rates. Similar trends were found in O6Na but with an initial capacity of 213 mAh/g. The lower capacities found in these oligomers, designed to have higher capacities, suggest that, although inactive, the intermediate aromatic ring between Schiff base functionalities that has been eliminated, may have a stabilizing effect either by favoring the π-π interactions or by avoiding N-N repulsions and loss of planarity.

The most remarkable result was the shift of the voltage plateau during discharge, at about 0.3V vs Na^+/Na in O6Na and 0.27V vs. Na^+/Na in O7Na. This lowering of voltage might be induced by N-N repulsions that may lower the voltage for further sodium insertion even below that for sodium plating. The useful lowering of voltage (still well above sodium plating) is of high importance since the material will be operating as an anode in a full cell and the lower the voltage of reduction vs $Na^+/Na^{0,}$ the higher the e.m.f. of the full cell ($V_{cell}=V_{cathode}-V_{anode}$) and the higher the resulting energy density (E_{cell}=Capacity × Voltage)..

Finally and in order to achieve the maximum reversible capacity for the oligomers with the higher capacities, electrodes containing 50% wt. KB and 50% wt. of the active material were prepared. (Figure S12). Reversible capacities of 320 mAh/g for O2Na and 340mAh/g for O5Na were delivered, which corresponds to 4.9 Na^+ and 7.59 Na^+ per oligomer unit or 2.45 and 2.59 Na^+ per Hückel active unit respectively. As these two oligomers contain the planar ending group and considering the carboxylic groups as possible active centers for Na^+, one Na^+ ion could be accommodated in each of the two carboxylic groups that both oligomers have. Interestingly, this will lead to a constant

value of 1.4 Na^+ per >C=N- moieties in both oligomers. Even though it is difficult to explain the insertion or extraction of such a value, it is in agreement with the result obtained in the poly-Schiff bases. Once again, the crystal structure and the interference with the electronic cloud of the phenyl groups, play an important role in the understanding of the storage mechanisms.

Given the low densities of the oligomers, (Table S5) these materials could be deployed in rechargeable batteries for applications were volume is not a constrain, such as stationary grid energy storage.

CONCLUSIONS

Crystalline oligomeric Schiff bases with carboxylate end groups have been synthesized from aromatics amines and aldehydes by simple condensation reaction. They present very promising electrochemical properties for anodes in sodium ion batteries (V< 1.5V vs. Na^+/Na). They have low hysteresis, capacities up to 340mAh/g at 21mA/g, coulombic efficiencies of >98% after few cycles, and capacity retentions of 92-97% after 25 cycles at C/10 and 84-92% after 25 cycles more at C/5. The maximum capacities are achieved for oligomers in which H^+ ions are replaced by Na^+ due to the fact that hydrogen bonding of the carboxylic end groups acting as crosslinks are removed and help to accommodate more easily inserted Na^+ ions.

The importance of the co-planarity between the different units within each oligomer is confirmed. Using DFT calculations we determined the "active" Hückel co-planar units for Na^+ insertion, which correspond to -$^-$OOC-ϕ-C=N- and-N=C-ϕ-C=N- groups, whereas the "non-active" units are the isoelectronic -$^-$OOC-ϕ-N=C and –C=N-ϕ-N=C- groups. In addition, we found a linear correlation between the number of inserted Na^+ ions and the number of active Hückel units. Therefore, the reversible capacity can be

directly related to the ratio between active/total Hückel units. Some other factors, such as crystallinity or electronic repulsions can also influence the reversible capacity, as no raise in capacity resulted when increasing the mentioned ratio. The electrochemical characterization has been performed on powders and therefore an improvement in the cycle life and rate capability is expected when measuring it in the form of thin films allowed from casting.

X-rays diffraction studies on the pristine oligomers would be helpful to get a deeper understanding of the system and are in progress.

Acknowledgments

The authors would like to thank Uxue Oteo for collecting BET data, Jon Ajuria for SEM characterization and Frederic Aguesse for discussing the impedance data. Funding through projects ENE2013-44330-R and Etortek 14 CICEnergiGUNE is acknowledged. M.L.H. acknowledges support from the European Master for Energy Storage and Conversion (MESC). J.C. acknowledges support by the Ramón y Cajal Fellowship, the Marie Curie Career Integration Grant FP7-PEOPLE-2011-CIG: Project NanoWGS, and The Royal Society through the Newton Alumnus scheme. Computer time provided by the Barcelona Supercomputer Center (BSC), i2BASQUE, and the Supercomputing Center of Galicia (CESGA) is acknowledged.

REFERENCES

[1] (a) Na-ion batteries, recent advances and present challenges to become low cost energy storage systems V. Palomares, P. Serras, I. Villaluenga, K. Hueso, J. Carretero-Gonzalez, T. Rojo, *Energy Envirom. Sci.*, **2012**, *5*, 5884. (b) Update on Na-based

battery materials. A growing research path V. Palomares, M. Casas-Cabanas, E. Castillo-Martinez, M. Han, T. Rojo, Energy and Envirom. Sci,, 2013, **6**, 2312.

[2] $Na_2Ti_3O_7$: Lowest Voltage Ever Reported Oxide Insertion Electrode for Sodium Ion Batteries P. Senguttuvan, G. Rousse, V. Seznec, J. M. Tarascon, M. R. Palacín *Chem. Mater.* , **2011**, *23*, 4109.

[3] *Carbon coated K0.8Ti1.73Li0.27O4: a novel anode material for sodium-ion batteries with a long cycle life.* K. Chen, W. Zhang, Y. Liu, H. Zhu, J. Duan, X. Xiang, L. Xue, Y. Huang. *Chem Comm.*, **2015**, *51*, 1608-1611.

[4] *Lepidocrocite-type layered titanate structures: New lithium and Sodium ion intercalation anode materials.* M. Shirpour, J. Cabana, M. Doeff, Chem Mater. **2014**, *26*, 2502-2512.

[5] *From biomass to a renewable LixC6O6 organic electrode for sustainable Li-ion batteries*. H. Chen, M Armand, G. Demailly, F.Dolhem, P. Poizot, J. M. Tarascon. *Chem. Sus. Chem.*, **2008**, *1*, 348.

[6] *Lithium salt of tetrahydroxybezoquinone: toward the development of a suitable Li-Ion Battery.* H. Chen, M. Armand, M. Courty,M. Jiang, C.P. Grey,F. Dolhem J. M. Tarascon, *J. Am. Chem. Soc*, **2009**, *131*, 8984.

[7] *Polyacetylene and Polyphenylene as Anode Materials for Non-aqueous Secondary Batteries* Shacklette, L. W., Toth, J.E., Murthy, N.S., Baughman, R.H., *J. Echem. Soc.* **1985**, *132*, 1529.

[8] *Conjugated dicarboxylate anodes for li-ion batteries*. M. Armand, S. Grugeon, H. Vezin, S. Laurelle, P. Ribiere, P. Poizot, J. M. Tarascon, *Nat. Mat.* **2009**, *8*, 120-125.

[9] *All Organic Sodium-Ion Batteries with Na4C8H2O6*. Shiwen Wang, Lijiang Wang, Zhiqiang Zhu, Zhe Hu, Qing Zhao, and Jun Chen., *Angew. Chem. Int. Ed.*, **2014**, *53*, 5892.

[10] *Sodium Terephthalate as an Organic Anode Material for Sodium Ion Batteries*. *Park, Y., Shin, D.-S., Woo, S. H., Choi, N. S., Shin, K. H., Oh, S. M., Lee, K. T. and Hong, S. Y., Adv. Mater.*, **2012**, *24*, 3562–3567.

[11] *Disodium Terephthalate ($Na_2C_8H_4O_4$) as High Performance Anode Material for Low-Cost Room-Temperature Sodium-Ion Battery*. Hao, L., Zhao, J., Hu, Y.-S., Li, H., Zhou, Z., Armand, M. and Chen, L., *Adv. Energy Mater.* **2012**, *2*: 962–965.

[12]Wang, C.; Xu, Y.; Fang, Y.; Zhou, M.; Liang, L.; Singh, S.; Zhao, H.; Schober, A.; Lei, Y.; "Extended π-conjugated systems for fast charge and discharge sodium ion batteries" *J. Am. Chem. Soc.* **2015**, *137*, 3124-30.

[13] A. Renault, V. A. Mihali, K. Edström, D. Brandell, "Stability of organic Na-ion battery electrode materials: The case of disodium pyromellitic diimidate" *Echem. Comm.*, **2014**, 52-55.

[14] M. Yao, K. Kuratani, T. Kojima, N. Takeichi, H. Senoh, T. Kiyobayashi "indigo carmine: an organic cyrstal as a positive electrode material for rechargeable sodium batteries. *Sci. Rep.*, **2014**, *4*: 3650.

[15] J. Hong, M. Lee, B. Lee, D.H. Seo, C.B. Park, K. Kang "Biologically inspired pteridine redox centres for rechargeable batteries" *Nature Comm.*, **2014**, *5*, 5335.

[16] *Poly-Schiff bases as low voltage redox centres for sodium ion batteries*. E. Castillo-Martínez, J. Carretero-González, M. Armand.: *Angew. Chem. Int. Ed.*, **2014**, *53*, 5445.

[17] P. Martinet, J. Simonet, J. Tendil, *"Courbes intensité-potentiel de quelques bases de Schiff dans le dimethylformamide anhydre"* ***Comp. Rend. Sci. Chem. Serie C*, 1969**, T269, 303-305.

[18] K. Deuchert, S. Hünig, "Multistage Organic Redox systems: A general structural principles" *Angew. Chem. Int. Ed.* , **1978**, *17*, 875-958.

[19] *Infrared Spectroscopy of Aqueous Carboxylic Acids: Comparison between Different Acids and Their Salts*. J.-J. Max, C. Chapados., *J. Phys. Chem A*, **2004**, *108*. 3324-3337.

[20] *Synthesis and characterization of some new Schiff base polymers*. Khuhawar, M.Y., Mughal, M.A., Channar, A.H., *Eur. Polym. J.*, **2004**, *40*, 805.

[21] J. Heinze, P. Tschuncky, A. Smie, *"The oligomeric approach –the electrochemistry of conducting polymers in the light of recent research"* *J. Solid State Electrochem.* **1998**, *2*, 102-109.

[22] J. C. Perez-Flores, C. Baehtz, M. Hoelzel, A. Kuhn and F. Garcia-Alvarado,"$H_2Ti_6O_{13}$, a new protonated titanate prepared by Li^+/H^+ ion exchange: synthesis, crystal structure and electrochemical Li insertion properties" *RSC Advances*, **2012**, *2*, 3530

[23] D. Banerjee, J. B. Parise, "Recent Advances in s-block metal carboxylate Networks" *Cryst. Growth Des.*, **2011**, *11*, 4704-4720.

[24] X. Han, C. Chang, L. Yuan, T. Sun, J. Sun "Aromatic carbonyl derivative polymers as high performance Li-ion battery materials" *Adv. Mater.* **2007**, *19*, 1616.

[25] Bürgi, H. B., Dunitz, J. D. "Crystal and Molecular Structures of Benzylideneaniline, Benzylideneaniline -p-carboxylic acid and *p* -Methylbenzylidene -*p* –nitroaniline " *Helvetica Chim. Acta*, **1970**, *53*, 1747-1764.

[26] Traetteberg, M., Hilmo, I., Abraham, R. J.; Ljunggren, The molecular structure of N-benzylidene-aniline, *J. Molec. Struct*, **1978**, *48*, 395-405.